JOURNAL OF SOLID STATE CHEMISTRY **124,** 169–175 (1996)
ARTICLE NO. 0221

Dependence of Pr^{3+} Distributions on the Composition of Pr^{3+}–β''-Alumina

Joachim Köhler and Werner Urland

Universität Hannover, Institut für Anorganische Chemie und Sonderforschungsbereich 173, Callinstraße 9, 30167 Hannover, Germany

Received August 22, 1995; in revised form February 28, 1996; accepted March 21, 1996

The structures of completely exchanged Na^+/Pr^{3+}–β''-Al_2O_3 crystals have been investigated by single crystal X-ray diffraction methods at room temperature. The ionic distributions within the conduction layers are correlated with the crystal compositions. A decreasing cation content in the layers increases the lattice parameter *c* connected with an expansion of the conduction slabs resulting in an increased Beevers–Ross (BR) site occupancy by Pr^{3+} ions. Up to 52% of the lanthanide ions are found to occupy the lower coordinated BR positions.

INTRODUCTION

The fast ion conductor Na^+–β''-Al_2O_3 is described in the case of Mg^{2+} stabilization by the formula $Na_{1+x}Mg_xAl_{10-x}O_{17}$. The stoichiometry varies over a wide range ($0.3 < x < 0.7$) with the idealized composition $Na_{1.67}Mg_{0.67}Al_{10.33}O_{17}$ (1–3). The compound crystallizes in the trigonal space group $R\bar{3}m$ and consists of alternating sequences of closed packed spinel blocks and loosely packed regions (the so-called conduction planes) containing the mobile Na^+ ions. Covalent linear Al–O–Al bonds and Coulomb attraction forces of the in-plane cations to the spinel block anions connect the blocks. Due to the high mobility an equivalent amount of the Na^+ ions is replaceable by other mono-, di-, and trivalent cations, especially by lanthanide ions (4, 5). Possible positions for the cations within the conduction slabs are the sevenfold coordinated Beevers–Ross (BR) sites (C_{3v} symmetry, 6*c* Wyckoff notation in $R\bar{3}m$) and the eightfold coordinated mid-Oxygen (mO) sites (C_{2h} symmetry, 9*d* notation). Resulting from the Coulomb interactions the Na^+ ions occupying neighbored BR positions are shifted in opposite directions toward the spinel block anions broadening the conduction slabs to a definite height H_1. Despite this three dimensional extension the designation as conduction plane is still often used in the literature indicating the similarity to the structure of Na^+–β-alumina (6). The Na^+ content within the conduction layers influences the lattice parameter *c* and the thickness of the conduction slabs (7).

A question always arises when describing the structure of β''-aluminas concerns the cation distribution within these slabs. For undoped Na^+–β''-Al_2O_3 a nonuniform Na^+ arrangement is reported giving the majority of the Na^+ ions within the BR (8, 9) or within the mO sites (10). In completely exchanged Na^+/Ln^{3+}–β''-Al_2O_3 crystals (*Ln* = lanthanide) the Ln^{3+} ions, especially the larger ones (*Ln* = Nd, Eu, Gd), mainly prefer the mO positions (up to 98% of the ion content) and only a minor fraction occupies the lower coordinated BR sites (11–13). Ln^{3+}–β''-Al_2O_3 isomorphs doped with smaller Ln^{3+} ions (e.g., Er^{3+}) show a BR occupancy of nearly 30% (14). Up to now, structural data determined by X-ray diffraction methods are available only for Na^+/Ln^{3+}–β''-alumina crystals corresponding to the aforementioned idealized composition $Ln_{0.56}Mg_{0.67}Al_{10.33}O_{17}$ (11–14).

In this paper the structures and ionic distributions of three completely exchanged Na^+/Pr^{3+}–β''-alumina crystals (degree of exchange: 94, 99, and 99%) varying in the cation content within the conduction planes are presented. The compositions of these crystals deviate from the stoichiometry reported so far and the cation distribution in the slabs is found to be strongly correlated with the Na^+ content of the utilized undoped Na^+–β''-alumina crystal (n_{Na_0}). With the given results inconsistencies in the literature concerning the ionic distributions and the resulting physical properties of lanthanide ion exchanged Na^+–β''-alumina can be understood.

EXPERIMENTAL

Na^+–β''-Al_2O_3 crystals (up to $7 \times 7 \times 3$ mm) have been grown by flux evaporation in a Na_2O rich flux (2). The characterization by electron probe microanalysis EPMA (Cameca CAMEBAX) led to an approximate composition $Na_{1+x}Mg_yAl_{11-y}O_{17}$ with $0.24 < x < 0.70$ and $0.25 < y < 0.77$ (15). Anhydrous $PrCl_3$ powder has been prepared by the ammonium chloride route (16). For the ion exchange the Na^+–β''-Al_2O_3 crystals were immersed under argon atmosphere in a $PrCl_3$ melt at 780°C for several hours. Generally, an exposure time of 2–3 h was sufficient for a

0022-4596/96 $18.00

TABLE 1
Experimental Parameters Related to the Data Collection and Structural Refinement of Completely Exchanged Na^+/Pr^{3+}–β''–Al_2O_3 Crystals

	Crystal I	Crystal II	Crystal III
Composition by microanalysis	$Na_{0.08\pm0.02}Pr_{0.44\pm0.02}Mg_{0.54\pm0.07}Al_{10.48\pm0.05}O_{17}$	$Na_{0.01\pm0.01}Pr_{0.51\pm0.01}Mg_{0.56\pm0.03}Al_{10.45\pm0.01}O_{17}$	$Na_{0.01\pm0.01}Pr_{0.53\pm0.04}Mg_{0.72\pm0.08}Al_{10.31\pm0.08}O_{17}$
Composition by refinement	$Na_{0.08\pm0.01}Pr_{0.43\pm0.02}Mg_{0.51\pm0.15}Al_{10.49\pm0.15}O_{16.93\pm0.13}$	$Pr_{0.50\pm0.02}Mg_{0.58\pm0.08}Al_{10.42\pm0.08}O_{16.96\pm0.05}$	$Pr_{0.53\pm0.01}Mg_{0.60\pm0.10}Al_{10.32\pm0.04}O_{16.88\pm0.06}$
Degree of exchange (%)	94	99	99
Cell parameters (298 K) (pm)	a = 561.1(5), c = 3347.9(27)	a = 561.2(4), c = 3339.7(25)	a = 563.1(2), c = 3334.2(15)
Space group, Z	$R\bar{3}m$, 3	$R\bar{3}m$, 3	$R\bar{3}m$, 3
ρ (X-ray) (g·cm^{-3})	3.471	3.501	3.488
Crystal dimensions (mm)	0.11 × 0.15 × 0.05	0.23 × 0.25 × 0.05	0.42 × 0.61 × 0.06
Diffractometer, radiation (pm)	STOE (AED-2) 4-circle, Mo$K\alpha$ (λ = 71.073)	STOE (AED-2) 4-circle, Mo$K\alpha$ (λ = 71.073)	STOE (AED-2) 4-circle, Mo$K\alpha$ (λ = 71.073)
R_{int}	8.99	10.18	7.11
Absorption correction	empirical	empirical	empirical
2Θ range	3.65° < Θ < 53.98°	2.05° < Θ < 58.07°	3.66° < Θ < 57.86°
h, k, l, range	±7, ±7, +42	±7, ±7, ±45	±7, ±7, ±45
Standard reflections	2 2 0, $\bar{4}$ 2 0, 2 0 20, 0 $\bar{2}$ 20	2 2 0, $\bar{4}$ 2 0, 2 0 20, 0 $\bar{2}$ 20	2 2 0, $\bar{4}$ 2 0, 2 0 20, 0 $\bar{2}$ 20
No. of observed reflections	1480	6671	3247
No. of unique reflections	296	358	356
Linear absorption factor (cm^{-1})	27.4	29.8	29.8
Refined parameters	49	49	49
Refinement	full-matrix least-squares, based on F^2	full-matrix least-squares, based on F^2	full-matrix least-squares, based on F^2
$R1$, $wR2$[a]	8.60, 19.27 (no σ-limit)	7.30, 16.32 (no σ-limit)	4.21, 10.83 (no σ-limit)
GooF = S[a]	1.107	1.273	1.194
Min., max. Δ ρ (e·pm^{-3}·10^{-6})	−0.74, 2.89	−1.19, 1.45	−0.45, 1.44
Program used	STRUCSY (20)[b], SHELXL-93 (21)	STRUCSY (20)[b], SHELXL-93 (21)	STRUCSY (20)[b], SHELXL-93 (21)

[a] Definition given in (21).
[b] Data reduction and intensity correction.

completely ion exchange (15). No further heat treatments were applied after quenching the crystals to room temperature. The crystal compositions and the degrees of exchange (ξ) were determined by EPMA. X-ray intensity measurements for crystal structure solution were performed at room temperature on a four-circle diffractometer (Siemens-Stoe, AED 2). Monitoring four representative standard reflections periodically during the measurements the exact crystal adjustments could be examined. The cell parameters were calculated from a selected set of 20 reflections being the same for each crystal. Some experimental parameters of the X-ray data collection are listed in Table 1. Conventional R factors based on F ($R1$) as well as weighted R factors based on F^2 ($wR2$) are given, respectively.

STRUCTURAL REFINEMENTS

The same refinement procedures were applied for the structure solutions of the three crystals. Initial parameters used in the least-squares refinements of the spinel blocks and the bridging oxygen ions were taken from Ref. (8). BR and mO positions were occupied with Pr^{3+} ions (Pr1 and Pr2, respectively). Due to the minor concentration a Na^+ occupancy could not be established in the refined models of the two 99% exchanged Na^+/Pr^{3+}–β''-Al_2O_3 crystals. For the 94% doped sample Na^+ occupancy was introduced for the BR sites. But due to the low scattering contributions of the minor concentrated Na^+ ions a definite localization of these ions among the heavier Pr^{3+} ions was not possible with the collected intensity data set. Therefore, the fractional atomic and displacement parameters of Na and Pr1 had to be equated and refined together. Nevertheless, the Na^+ site occupation factor was determined without any constraint. Alternative refinements with Na^+ in mO sites led to unreasonable site occupation factors and to increased R values. This ionic contribution (Na^+ in mO) was not considered for further discussions.

Finally, the bridging oxygen ions O(5) of all crystals were displaced into 18g sites slightly shifted from the 3b positions Al^{3+} and O^{2-} in the spinel blocks were refined independently without any constraint. Those sites showing full occupancies were subsequently fixed in the final refinements. Due to the nearly equal atomic form factors Mg^{2+} and Al^{3+} ions within the spinel blocks were not distinguishable. Because of charge neutrality the Mg^{2+} content could be estimated from the refined cationic/anionic occupancy ratio. Attempts were made to refine the structures in the noncentrosymmetric space group $R3m$ but no significant improvements of the residual R factors were observed.

The final atomic parameters, equivalent displacement factors, and some interatomic distances of the refined models are listed in Table 2 and 3, respectively. The average electron distribution (ρ_{obs} map) in the conduction plane (z = 0.17) is given for each crystal in Fig. 1, respectively.[1]

RESULTS AND DISCUSSION

The structure of the spinel blocks (Mg/Al distributions, vacancies, etc.) is similar to other β''-aluminas studied be-

[1] Further details of the crystal structure investigations can be requested at the FACHINFORMATIONS ZENTRUM KARLSRUHE, 76344 Eggenstein-Leopoldshaten 2, by giving the deposit numbers: CSD 404 216 (crystal I), CSD 404 254 (crystal II), CSD 404 218 (crystal III).

TABLE 2

Site Multiplicities, Occupation Factors, Fractional Atomic Coordinates, and Equivalent Displacement Parameters (pm^2) for $Na_{0.08}Pr_{0.44}Mg_{0.54}Al_{10.48}O_{17}$ (upper row), $Na_{0.01}Pr_{0.51}Mg_{0.56}Al_{10.45}O_{17}$ (middle row), and $Na_{0.01}Pr_{0.53}Mg_{0.72}Al_{10.31}O_{17}$ (lower row)

Atom	Site	s.o.f.	*x*/*a*	*y*/*b*	*z*/*c*	U_{eq}[a]
Pr(1)	6*c*	0.110(4)	0	0	0.1749(2)	204(27)
		0.059(4)	0	0	0.1756(5)	317(44)
		0.011(2)	0	0	0.1756(26)	855(228)
Na	6*c*	0.040(2)	0	0	0.1749(2)	204(27)
		—	—	—	—	—
		—	—	—	—	—
Pr(2)	9*d*	0.068(6)	0.8333	0.1667	0.1667	280(42)
		0.126(3)	0.8333	0.1667	0.1667	268(16)
		0.169(2)	0.8333	0.1667	0.1667	231(6)
Al(1)	3*a*	1.0	0	0	0	17(12)
		1.0	0	0	0	64(1)
		1.0	0	0	0	72(4)
Al(2)	6*c*	0.996(19)	0	0	0.3504(1)	28(10)
		1.0	0	0	0.3503(1)	84(6)
		1.0	0	0	0.3502(4)	90(4)
Al(3)	18*h*	1.0	0.3349(4)	0.5*x*	0.0717(1)	27(8)
		1.0	0.3352(3)	0.5*x*	0.0718(1)	91(6)
		0.986(6)	0.3346(1)	0.5*x*	0.0719(1)	78(4)
Al(4)	6*c*	1.0	0	0	0.4509(1)	36(10)
		1.0	0	0	0.4510(1)	85(7)
		1.0	0	0	0.4503(1)	84(4)
O(1)	18*h*	0.989(21)	0.1542(5)	2*x*	0.0349(1)	44(16)
		1.0	0.1545(4)	2*x*	0.0347(1)	110(9)
		0.979(9)	0.1540(2)	2*x*	0.0347(1)	102(6)
O(2)	6*c*	1.0	0	0	0.2949(2)	45(18)
		1.0	0	0	0.2952(2)	71(13)
		1.0	0	0	0.2947(1)	83(6)
O(3)	6*c*	1.0	0	0	0.0975(2)	49(19)
		1.0	0	0	0.0978(2)	87(14)
		1.0	0	0	0.0983(1)	114(7)
O(4)	18*h*	1.0	0.1639(4)	2*x*	0.2347(1)	40(12)
		1.0	0.1635(3)	2*x*	0.2348(1)	77(9)
		1.0	0.1632(2)	2*x*	0.2344(1)	96(5)
O(5)	18*g*	1.0	0.4228(72)	0.6667	0.1667	191(164)
		0.956(50)	0.4142(39)	0.6667	0.1667	143(65)
		1.0	0.4117(32)	0.6667	0.1667	149(62)

[a] $U_{eq} = 1/3\ [U_{33} + 4/3\ (U_{11} + U_{22} - U_{12})]$ (22).

fore and will therefore not be discussed in further detail. The ion distribution within the conduction planes (*ab*-planes) is of main interest.

The three investigated crystals are characterized by their composition given in Table 1 (the Pr^{3+} content amounts to 0.44 (crystal I), 0.51 (crystal II), and 0.53 (crystal III) per formula unit). The incorporation of Pr^{3+} ions into Na^+–β''-Al_2O_3 leads to a reduction of the lattice parameter *c* caused by the smaller ionic radius and the stronger Coulomb attraction forces to the spinel block anions (c = 3385 pm for undoped Na^+–β''-Al_2O_3 (8)). On the other hand, the lattice parameter *a* is determined by the dimensions of the rigid spinel blocks and remains nearly uneffected by the ion exchange (561.4 pm for Na^+–β''-Al_2O_3 (8)). The crystal compositions are refined to $Na_{0.08\pm0.01}Pr_{0.43\pm0.02}Al_{10.99\pm0.04}O_{16.93\pm0.13}$ (crystal I), $Pr_{0.50\pm0.02}Al_{11.00}O_{16.96\pm0.05}$ (crystal II), and $Pr_{0.53\pm0.01}Al_{10.92\pm0.04}O_{16.88\pm0.06}$ (crystal III) having a negative deficit of 0.51 ± 0.15 (I), 0.58 ± 0.08 (II), and 0.60 ± 0.10 (III) electrons per formula unit, respectively. From neutron diffraction measurements on Mg^{2+} stabilized Na^+–β''-Al_2O_3 crystals it is known that Mg^{2+} substitutes Al^{3+} at the tetrahedral Al(2) site close to the centers of the spinel blocks (10). Hence, attributing the charge disproportion to Mg^{2+} the compositions result after substraction from the Al^{3+} content in $Na_{0.08\pm0.01}Pr_{0.43\pm0.02}Mg_{0.51\pm0.15}Al_{10.48\pm0.05}O_{16.93\pm0.13}$ (I), $Pr_{0.50\pm0.02}Mg_{0.58\pm0.08}Al_{10.42\pm0.08}O_{16.96\pm0.05}$ (II), and $Pr_{0.53\pm0.01}Mg_{0.60\pm0.10}Al_{10.32\pm0.04}O_{16.88\pm0.06}$ (III) in reasonable agreement with the microprobe analysis

TABLE 3
Selected Interatomic Distances (pm) in $Na_{0.08}Pr_{0.44}Mg_{0.54}Al_{10.48}O_{17}$ (upper row), $Na_{0.01}Pr_{0.51}Mg_{0.56}Al_{10.45}O_{17}$ (middle row), and $Na_{0.01}Pr_{0.53}Mg_{0.72}Al_{10.31}O_{17}$ (lower row)

Pr(1)–O(5)	(3×)	283.0(33)	Al(2)–O(1)	(3×)	184.1(5)
		287.2(18)			183.7(4)
		289.3(18)			184.8(2)
Pr(1)–O(4)	(3×)	255.9(7)	Al(2)–O(2)	(1×)	185.6(9)
		253.7(12)			184.1(7)
		252.5(68)			185.0(4)
Pr(1)–O(3)	(1×)	259.3(11)	Al(3)–O(4)	(2×)	183.8(3)
		259.7(17)			183.4(2)
		257.6(88)			184.2(1)
Pr(2)–O(5)	(2×)	230.4(41)	Al(3)–O(3)	(1×)	184.1(4)
		235.2(22)			184.7(3)
		237.4(19)			185.4(2)
Pr(2)–O(4)	(4×)	278.8(4)	Al(3)–O(2)	(1×)	196.1(5)
		278.4(3)			196.4(4)
		277.2(2)			196.3(2)
Pr(2)–O(3)	(2×)	282.7(6)	Al(3)–O(1)	(2×)	199.4(4)
		281.2(5)			199.9(3)
		279.9(3)			200.1(2)
Al(1)–O(1)	(6×)	190.0(5)	Al(4)–O(5)	(1×)	172.0(12)
		189.7(4)			171.8(7)
		189.6(2)			171.6(5)
			Al(4)–O(4)	(3×)	176.4(4)
					177.0(3)
					176.4(2)

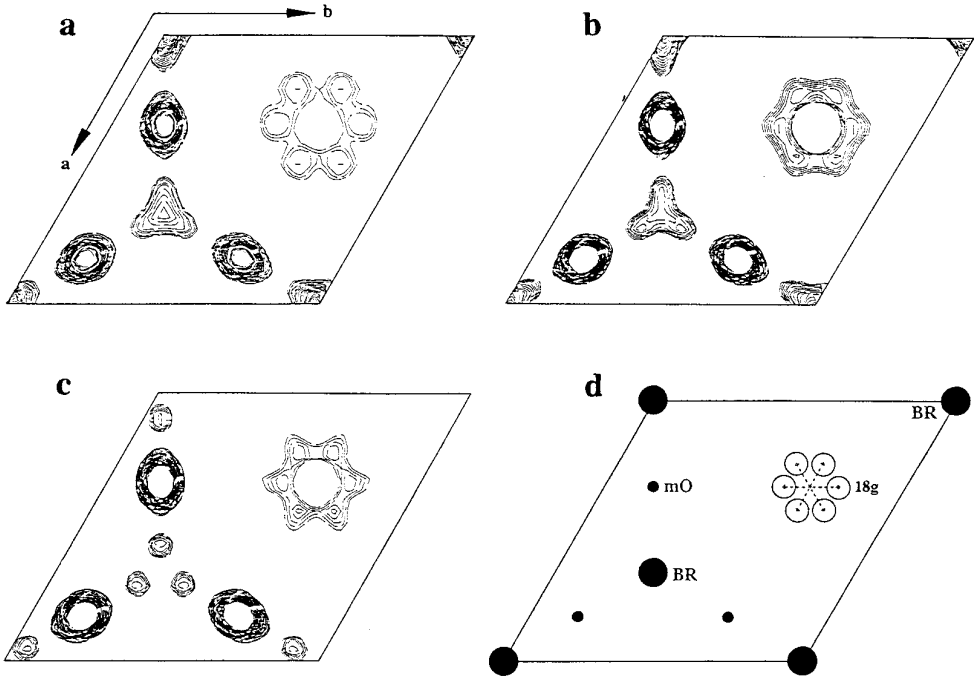

FIG. 1. Electron density map (ρ_{obs}) of the conduction planes ($z = 0.17$) in (a) $Na_{0.08}Pr_{0.44}Mg_{0.78}Al_{10.36}O_{17}$ ($\xi = 94\%$), (b) $Na_{0.01}Pr_{0.51}Mg_{0.56}Al_{10.45}O_{17}$ ($\xi = 99\%$), and (c) $Na_{0.01}Pr_{0.53}Mg_{0.72}Al_{10.31}O_{17}$ ($\xi = 99\%$) (compositions determined by EPMA). The contour intervals are 2 $eÅ^{-3}$. A schematic representation of the occupied sites is given in (d).

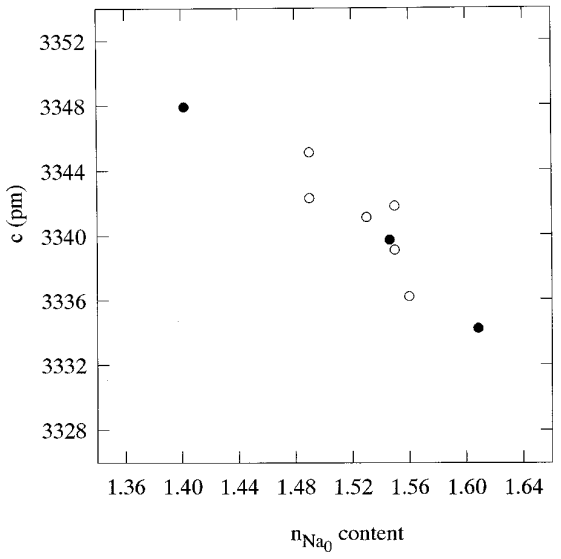

FIG. 2. Lattice parameter c (pm) of completely exchanged Na^+/Pr^{3+}–β''-Al_2O_3 crystals as a function of the original Na^+ content per formula unit, n_{Na_0} (○). Values of the three Na^+/Pr^{3+}–β''-Al_2O_3 crystals presented within this work are given by solid symbols (●).

given in Table 1. As can be seen from Fig. 1 the electron density is extended for all positions in the conduction planes indicating large local disordering induced by Coulomb interactions between the ions. Pr^{3+} ions occupying mO sites are shifted toward neighbored empty BR positions. Cations within BR sites displace in direction of spinel block oxygen ions (z-direction) and show additionally large in-plane components of the anisotropic displacement factors toward 18h sites caused by the repulsion of cations in adjacent occupied positions. The sites of the column oxygens O(5) are influenced by the local cation environment and split into six disordered 18g sites slightly displaced from the 3b positions (occupied in undoped Na^+–β''-alumina). Due to the space and time averaging in X-ray measurements all individual ionic shifts in the conduction planes are integrated resulting in the extended electron density regions around each mean position as indicated by the large thermal displacement parameters in the refined models (see Table 2).

From Table 1 it can be seen that an increasing Pr^{3+} content is connected with a decreasing c-lattice extension explainable by the growing cationic attraction effects between the repelling spinel blocks. This dependence (in-plane cation content versus the cell parameter c) is shown in Fig. 2. X-ray data of completely exchanged Na^+/Pr^{3+}–β''-Al_2O_3 crystals investigated in addition are added for confirmation (15). For better elucidation the cell parameters are plotted versus the original Na^+ content per formula unit of the employed undoped Na^+–β''-alumina crystals (n_{Na_0}). n_{Na_0} is calculated from the composition of the exchanged crystals by adding up the Na^+ and the triple Pr^{3+} content ($n_{Na_0} = n_{Na^+} + 3n_{Pr^{3+}}$). The cell shrinkage (in c direction) of Na^+/Pr^{3+}–β''-alumina results in the formation of a bent Al–O–Al bridge leading to shortened Pr–O(5) distances (see Table 3). Interestingly, the O(5) displacements (50.2 pm in crystal I, 45.4 pm in II, and 44.1 pm in III) toward occupied mO and BR positions are lowered with growing in-plane cation content despite the decreasing cell parameter c (3347.9(27) pm for I, 3339.7(25) pm for II, and 3334.2(15) pm for III). The Pr^{3+} concentration in the conduction planes seems to be the important parameter rather than the cell dimensions (c value) to influence the O(5) displacements. More cations around a bridging oxygen ion have a compensating effect on the O(5) shifts by additional attraction forces in opposite directions.

Turning to the feature of main interest, the lanthanide ion distribution in the planes, it is important to note that the Pr^{3+} ions occupy the lower coordinated BR positions to a significant extent (52% in crystal I, 24% in II, and 6% in III) in contradiction to X-ray studies of completely exchanged Na^+/Ln^{3+}–β''-Al_2O_3 crystals, published so far (11–13). For comparison, in the Nd^{3+} isomorph ($r_{Nd^{3+}}$ = 110.9 pm, $r_{Pr^{3+}}$ = 112.6 pm for coordination number CN = 8; cf. r_{Na^+} = 118.0 pm (17)) only 5% of the lanthanide ions are located in BR sites (13). From Table 2 a correlation of the Pr^{3+} content with the ionic distribution is recognizable. An increased Pr^{3+} concentration induces lowered BR site occupancy. For an interpretation of this effect the crystal compositions, especially of the employed undoped Na^+–β''-Al_2O_3 crystals (n_{Na_0}), have to be considered. Figure 3 displays the dependence of the Na^+ concentration on the

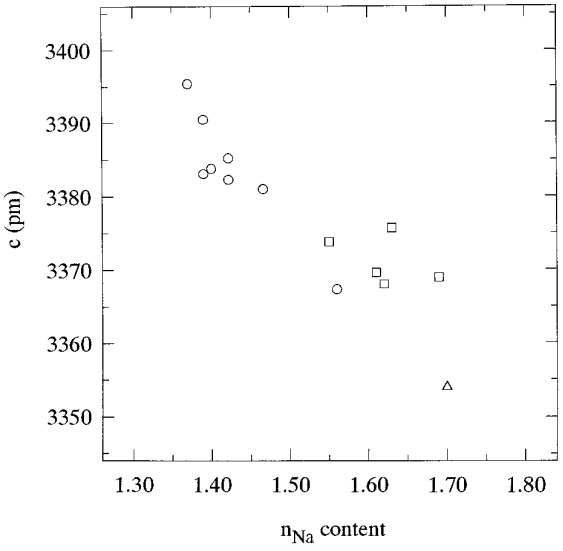

FIG. 3. Lattice parameter c (pm) of undoped Na^+–β''-Al_2O_3 crystals as a function of the Na^+ content per formula unit, n_{Na} (○) (compositions determined by EPMA). Corresponding literature data are included for comparison (△ (9), □ (1, 18)).

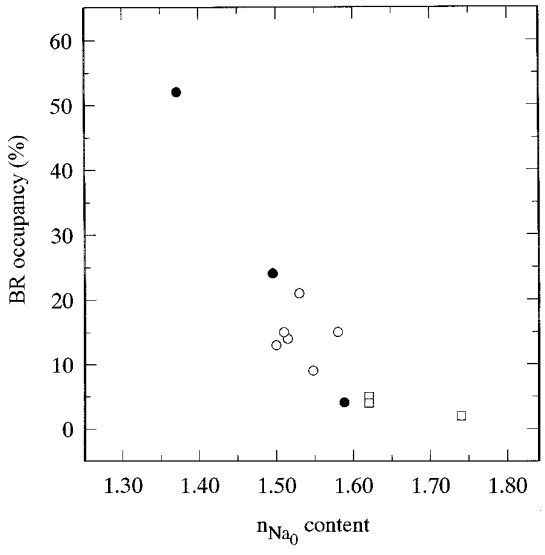

FIG. 4. BR site occupancy by Pr^{3+} ions (%) as a function of the original Na^+ content per formula unit, n_{Na_0} (○). Values of the three Na^+/Pr^{3+}–β''-Al_2O_3 crystals presented within this work are given by solid symbols (●). Corresponding data for Ln^{3+}–β''-Al_2O_3 crystals (Ln = Nd, Eu, Gd) (13) are added for comparison (□). All n_{Na_0} data are referred to the refined crystal compositions.

lattice parameter c of several pure Na^+–β''-Al_2O_3 crystals varying in composition. These data are in accordance with the linear correlation given in an earlier work by Harbach (7). With decreasing number of Na^+ ions within the planes the cell parameter c is increased equivalent to an expansion of the conduction slabs as already mentioned for the Pr^{3+} content in Pr^{3+}–β''-alumina (see Fig. 2). In Fig. 4 the dependence of the BR site occupancy by Pr^{3+} ions on the original Na^+ content (n_{Na_0}) of the used pure Na^+–β''-Al_2O_3 crystals is shown. The results of X-ray investigations of other completely exchanged Na^+/Pr^{3+}–β''-Al_2O_3 crystals are included for confirmation (15). Corresponding values of Ln^{3+}–β''-Al_2O_3 crystals (Ln = Nd, Eu, Gd) are added (13). To compare with these literature data for which no analytical composition was given the n_{Na_0} values are referred to the refined crystal compositions (see Table 1 and Ref. (13)). It can be stated that a decreased cation concentration (n_{Na_0}) leads to a raised BR occupancy by the lanthanide ions. Using Na^+–β''-Al_2O_3 crystals with small Na^+ concentration ($n_{Na_0} < 1.40$ per formula unit (FU)) for the ion exchange the Pr^{3+} ions can easily diffuse through the widened slabs occupying BR and mO positions to a nearly equal extent. With decreasing thickness of the slabs (1.40/FU $< n_{Na_0} <$ 1.60/FU) the Pr^{3+} mobility is restricted and a preference for the more spacious mO sites occurs. Finally, in Na^+–β''-Al_2O_3 crystals with $n_{Na_0} >$ 1.60/FU an exclusive mO occupancy by the lanthanide ions after the exchange procedure results due the narrowness of the slabs. A similar result is found for a Nd^{3+}–β''-Al_2O_3 crystal with the composition $Na_{0.01}Nd_{0.50}Mg_{0.44}Al_{10.55}O_{17}$. X-ray measurements indicate a BR occupancy by Nd^{3+} ions of about 20% (15) in comparison to 5% for a crystal having the composition $Nd_{0.54}Mg_{0.62}Al_{10.38}O_{17}$ (13). An interesting feature of Fig. 4 is the significant increase of BR occupancy for crystals with $n_{Na_0} <$ (1.55–1.60)/FU. The corresponding height of the conduction slabs (H) is correlated to the n_{Na_0} concentration and can be deduced by a simple equation (7) to 254–256 pm. In more widened slabs the Pr^{3+} ions are assumed to become mobile and to occupy the smaller BR positions. These results are confirmed by impedance spectroscopic measurements on Na^+/Pr^{3+}–β''-Al_2O_3 crystals where H can be determined in reasonable agreement to 253–254 pm. The raised Pr^{3+} mobility results in an increased ionic conductivity (19).

The spacing of the conduction slabs is an important controlling factor for the ionic distribution within the planes. This behavior agrees with the observation that excessive heat treatments at 1000°C induce BR occupancy in Eu^{3+}–β''-alumina (12). At this temperature the slabs are widened by thermal vibrations and the increased Eu^{3+} mobility leads to a partial BR occupancy.

CONCLUSIONS

In Na^+/Pr^{3+}–β''-Al_2O_3 differing in crystal composition an enhancement of the degree of BR site occupancy with decreasing cation content is observed. This is due to the increased spacings of the conduction slabs as the cation content becomes smaller. Based on this, a strong correlation between crystal composition, lattice constants, and ionic distributions within the conduction layers is found in completely exchanged Na^+/Pr^{3+}–β'' alumina. With the knowledge of one of these three parameters the remaining two can be predicted without any further information.

ACKNOWLEDGMENTS

We thank Dr. J. Koepke for the analytical measurements and the Deutsche Forschungsgemeinschaft for financial support.

REFERENCES

1. M. Aldén, *Solid State Ionics* **20,** 17 (1986).
2. F. Tietz, J. Koepke, and W. Urland, *J. Cryst. Growth* **118,** 314 (1992).
3. N. Weber and M. Bettman; quoted in J. T. Kummer, *Prog. Solid Chem.* **7,** 141 (1972).
4. B. Dunn and G. C. Farrington, *Solid State Ionics* **9/10,** 223 (1983).
5. S. Sattar, B. Ghosal, M. L. Underwood, H. Mertwoy, M. A. Saltzberg, W. S. Frydrych, G. S. Rohrer, and G. C. Farrington, *J. Solid State Chem.* **65,** 231 (1986).
6. J. T. Kummer, *Prog. Solid State Chem.* **7,** 141 (1972).
7. F. Harbach, *J. Mater. Sci.* **18,** 2437 (1983).
8. M. Bettman and C. R. Peters, *J. Phys. Chem.* **73,** 1774 (1969).
9. J. P. Boilot, G. Collin, P. Colomban, and R. Comes, *Phys. Rev. B* **22,** 5912 (1980).

10. G. M. Brown, D. A. Schwinn, J. B. Bates, and W. E. Brundage, *Solid State Ionics* **5,** 147 (1981).
11. W. Carrillo-Cabrera, J. O. Thomas, and G. C. Farrington, *Solid State Ionics* **9/10,** 245 (1983).
12. W. Carrillo-Cabrera, J. O. Thomas, and G. C. Farrington, *Solid State Ionics* **18/19,** 645 (1986).
13. W. Carrillo-Cabrera, J. O. Thomas, G. C. Farrington, *Solid State Ionics* **28/30,** 317 (1988).
14. M. Wolf and J. O. Thomas, *J. Mater. Chem.* **4,** 839 (1994).
15. J. Köhler, Ph.D. Thesis, University of Hannover (1996).
16. G. Meyer, *Inorg. Synth.* **25,** 146 (1989).
17. R. D. Shannon, *Acta Crystallogr. Sect. A* **32,** 751 (1976).
18. M. Aldén, J. O. Thomas, and P. Davies, *Solid State Ionics* **18/19,** 694 (1986).
19. J. Köhler and W. Urland, *Z. Anorg. Allg. Chem.* **622,** 191 (1996).
20. Siemens-Stoe, ''STRUCSY, Program Package for Crystal Structure Solution.'' Darmstadt.
21. G. M. Sheldrick, ''SHELXL-93, A Program for Crystal Structure Refinement.'' Universität Göttingen, 1993.
22. R. X. Fischer and E. Tillmanns, *Acta Crystallogr. Sect. C* **44,** 775 (1988).